

## Supplementary Information

### Surfaces Enhanced Film-Coupled Silver Nanopolyhedrons for Optical Transmittance

Xiuhui Bai,<sup>a</sup> Jigang Wang,<sup>a</sup> Ming Guo,<sup>a</sup> Zhen Li,<sup>a</sup> Ning Chen,<sup>a</sup> Qiang Wang,<sup>\*a</sup> Chunhong Li,<sup>b</sup> Changzheng Wang,<sup>\*c</sup> Kun Dong<sup>c</sup> and Shaowei Chen<sup>\*d</sup>

---

<sup>a</sup> *Laboratory for Micro-sized Functional Materials & College of Elementary Education and Department of Chemistry, Capital Normal University, Beijing, 100048, P.R. China.*

<sup>b</sup> *Beijing National Laboratory for Condensed Matter Physics, Institute of Physics, Chinese Academy of Sciences, P.O. Box 603, Beijing 100190, China.*

<sup>c</sup> *Key Laboratory of Urban Stormwater System and Water Environment, Ministry of Education, Beijing University of Civil Engineering and Architecture, Beijing, 100044, P. R. China.*

<sup>d</sup> *Department of Chemistry and Biochemistry, University of California, Santa Cruz, CA 95064, USA.*

*\*Corresponding author. E-mail: qwchem@gmail.com; changzhwang@163.com; shaowei@ucsc.edu.*

## **Table of Contents**

### **S1. Synthesis of silver nanopolyhedrons.**

#### *S1.1 Materials*

#### *S1.2 Synthesis of silver NPs*

#### *S1.3 Synthesis mechanism*

#### *S1.4 Morphology evolution with the different reaction time.*

#### *S1.5 Influence of the additive of zinc.*

#### *S1.5 SEM of silver nanopolyhedrons with different reaction times.*

### **S2. Effective indices of gap modes**

### **S3. Scanning electronic microscopy images of surface coverage**

Herein we report a further improved polyol approach to obtain monodispersed Ag NPs in an EG-based polyol system with zinc as the additive or promoter at 140 °C. We demonstrate that we can drastically improve the production rate of silver NPs by adding a trace amount of zinc. The success of this synthesis relies on a tight control over the nucleation process through the addition of trace amounts of zinc, as well as the use of PVP as an effective capping agent for small-sized particles. As far as I'm concerned, the addition of Zn will catalyze the reduction of Ag<sup>+</sup> in a mechanism analogous to the autocatalytic reduction of AgNO<sub>3</sub> through a galvanic replacement reaction. As a result, we were able to effectively limit the formation of twinned seeds and minimize the size distribution of resultant single-crystal NPs with the approximate same size.

#### *S1.1 Materials*

Ethylene glycol (A.R.), PVP ( $M_r \approx 58\ 000$ ), NaCl ( $\geq 99.8\%$ , A.R.), AgNO<sub>3</sub> ( $\geq 99.8\%$ , A.R.), and Zn ( $\geq 90\%$ , A.R.). All of the materials and reagents were used directly without further purification. Distilled water was purified with a Milli-Q system (Millipore, Billerica, MA). A stirring hotplate with a temperature controller (Ms7-H550-Pro, Dragon Laboratory Instruments limited), and micropipettes (Eppendorf Research<sup>R</sup> Plus) were used.

### ***S1.2 Synthesis of silver NPs***

In a typical synthesis, 5 mL of ethylene glycol was held in a 20 mL glass vial and heated in an oil bath at 140 °C under magnetic stirring for 1 h. NaCl (1 ml of 0.25 mM in EG) was then quickly added. After about 10 minutes, suspension of zinc (60  $\mu$ l of 0.09 g in 5 ml EG) was added to the solution. After at least 5 min, AgNO<sub>3</sub> (3 ml of a 99.13 mM solution in EG) and poly(vinyl pyrrolidone) (PVP, 3 ml of a solution in EG (312 mM in terms of the repeating unit,  $M_r \approx 58\ 000$ )) were simultaneously added to the stirring solution. The NPs were obtained by quenching the reaction with an ice-water bath when the reaction procedure was finished in 3.5 h. All samples for morphology and structure analysis were washed with acetone and then with water three times to remove excess EG and PVP.

### ***S1.3 Synthesis mechanism***

In principle, as we all know, there are two different pathways for Ag atoms to nucleate: homogeneous and heterogeneous. Homogeneous nucleation necessitates the presence of a supersaturated concentration of free Ag atoms, which can be obtained

through steady reduction of a salt precursor. Once supersaturation has been achieved, the free Ag atoms coalesce into small clusters, which then serve as nuclei for further growth. The nucleation process could be quenched until the concentration of Ag atoms below the supersaturation threshold because of the consumption of the available Ag atoms. In contrast, heterogeneous nucleation is characterized by the deposition of Ag atoms on locally available surfaces, without requiring a supersaturated environment. This is due to an intrinsically lower free energy barrier for heterogeneous nucleation as compared to homogeneous nucleation, providing a theoretical basis for rapid synthesis of metal nanoparticles.

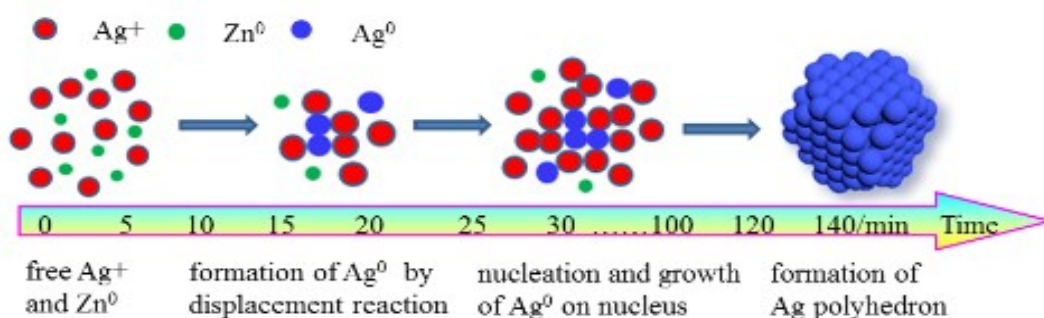
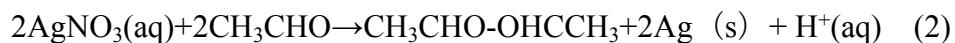


Fig. S1. Schematic illustration showing the synthesis of Ag NPs through heterogeneous nucleation and growth on silver clusters generated by the galvanic replacement reaction. The small silver clusters are immediately formed upon the introduction of AgNO<sub>3</sub>, followed by the deposition of Ag<sup>0</sup> atoms to yield Ag NPs.

In this reaction, the presence of zinc greatly accelerated the polyol synthesis of silver NPs due to a dramatic increase in the nucleation rate of silver ions. The initial Ag nanoparticles are obtained via the galvanic replacement reaction in the presence of poly(vinyl pyrrolidone)(PVP) compared to the reduction by ethylene glycol in the typical polyol synthesis as shown in eqns (1) and (2).



Beyond question, the displacement response is faster than reduction reaction. Based on this information, the  $\text{Ag}^0$  generated justly by replacement reaction, serve as sites for rapid heterogeneous nucleation and growth. The number of these nucleation sites will determine the size of the final Ag NPs, since the fixed number of Ag atoms available from the precursors are supposed to be evenly divided among the nuclei during growth. These conditions result in fast nucleation and growth of the silver seeds, and may therefore have reduced the time available for twin defects to form. Thus, a larger number of nuclei will produce smaller Ag nanocrystals, and vice versa. The newly formed twinned crystals were etched by  $\text{Cl}^-/\text{O}_2$ , and only single-crystals were left. The higher the concentration of  $\text{Ag}^+$ , the faster the single-crystals will come into being. As a result, uniform Ag NPs with Small size could be rapidly prepared in an EG-based system containing a trace amount of zinc.

Fig.S2A demonstrates the SEM images of Ag NPs by improved polyol strategy in the presence of zinc as the additive or promoter, and the corresponding extinction spectrum was described in Fig.S2B. As we can see, the products are consisted of a large quantity of silver NPs with uniform with corners. The samples showed an absorption band at about 450 nm, and the number of peaks and relative positions are consistent with theoretical calculation.

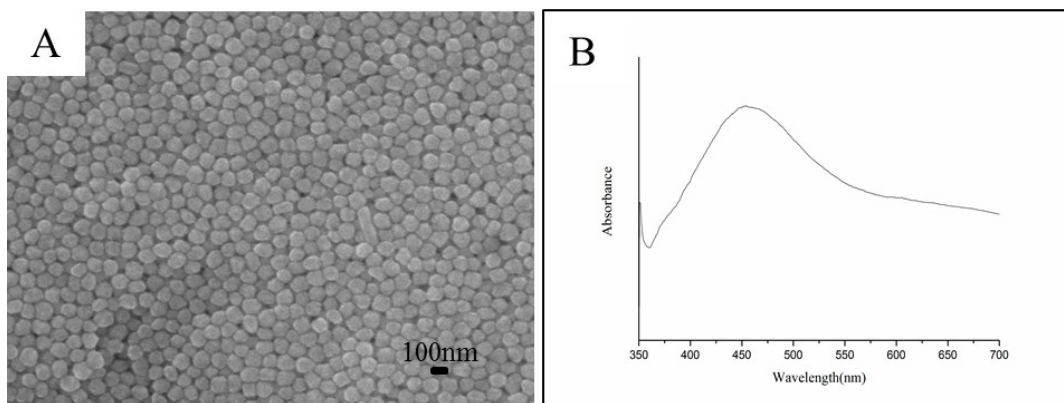


Fig.S2. (A) SEM image of a typical sample of Ag NPs taken at 3.5 h synthesized by the zinc modified polyol methods. (B) The extinction spectrum of the Ag NPs.

#### ***S1.4 Morphology evolution with the different reaction time.***

There was little change upon injection of suspension of zinc, a catalyst for the generation of nuclear of silver. During the synthesis, we could easily monitor the progress of the nanoparticle production through its color changes and then characterize the evolution of shape using scanning electron microscopy (SEM). Fig.S3 shows SEM images of samples taken at different stages of a typical synthesis. The solution turned milky white at the point of 2 min, and this indicates the presence of AgCl (Fig. S3A). The solution turned bright yellow at about 15 min, which indicates that large AgCl nanoparticles dissolved because of the initially formed Ag nanoparticles appeared (Fig. S3B). The solution started darkening from a bright yellow to a deep orange due to the growth of small silver particles. (Fig. S3C, D)

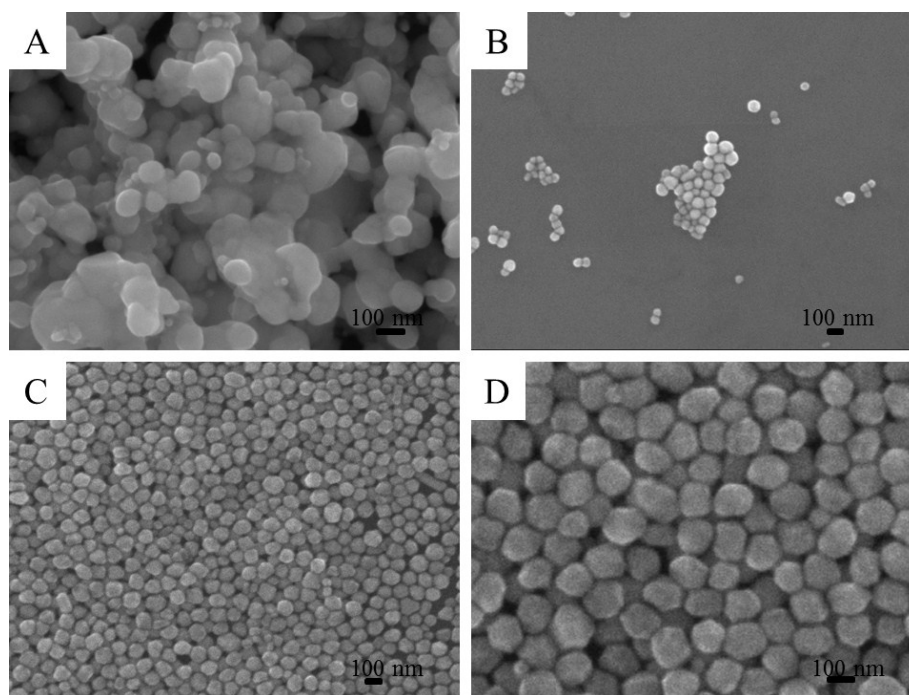


Fig. S3. Morphology evolution with the different reaction time. (A)  $t = 2$  min, (B)  $t = 15$  min, (C)  $t = 100$  min and (D)  $t = 200$  min. SEM images of the silver nanoparticles contained in the corresponding reaction solution shown.

### ***S1.5 Influence of the additive of zinc.***

In order to further verify the key role of zinc, a great deal of work has been done. Fig. S4 shows the SEM images of product conducted under the same reaction conditions except that the concentration of zinc in the EG solution was increased from 0 to 100  $\mu$ l. As we can see, under different conditions, different products were synthesized. For example, there will be some irregular nanoparticles and silver nanowires if we don't add zinc. (Fig. S4A) It was found that the ideal concentration of Zn to obtain Ag NPs with good uniformity and in large quantities is 60  $\mu$ l among these serial experiments. The emergence of irregular Ag nanoparticles in some of the products (shown in Fig. S4B, C) may probably be owing to the low concentration of zinc

nanoparticles. All zinc atoms may be oxidized to  $Zn^{2+}$ , we guess, or it is too little to work for the rapid emergence of nucleus. As a result, the galvanic replacement reaction will be restricted and single twinned could be generated. Meanwhile, it is important to note that adding too much zinc will play a side effect as shown in Fig.S4 E, F. It is believed that the high concentration of zinc leads to a so quickly growth process that resulting in the forming of big or irregular NPs. The more Ag atoms in the unit volume exist, the more rapid of the formation of Ag NPs is, and so the bigger or more irregular Ag NPs would come into being. Ideally, we wished that Zn atomic and free  $Ag^+$  ions quickly react to produce highly Ag NPs, which then serve as sites for the rapid heterogeneous nucleation of Ag atoms and subsequent formation of single-crystal NPs. The number of these nucleation sites will determine the size of the final Ag NPs, since the fixed number of Ag atoms available from the precursors are supposed to be evenly divided among the nuclei during growth. Thus, a larger number of nuclei will produce smaller AgNPs (Fig. S4D), and vice versa.

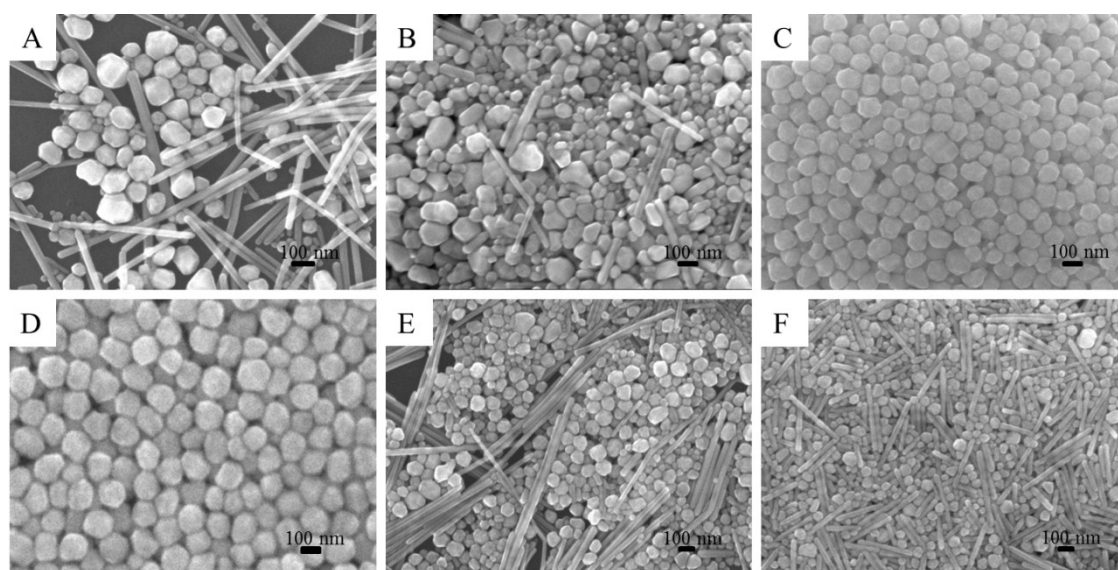


Fig. S4. SEM images of Ag nanoparticles synthesized with different concentrations of



Zn in the improved polyol synthesis. (A) 0 ul, (B) 20ul, (C) 40ul, (D) 60ul, (E)80ul, (F) 100ul. The solution was composed of AgNO<sub>3</sub> (24.75 mM) and PVP (38.75 mM, calculated in terms of the repeating unit), NaCl (0.25 mM), and was heated in an oil bath held at 140°C.

### ***S1.5 SEM of silver nanopolyhedrons with different reaction times.***

We have synthesized Ag NPs with the additive or promoter of Zn. Fig.S5 shows the images of the Ag NPs. As illustrated in Fig.S5A, Ag NPs were synthesized at 140°C with an agitation speed of 800 rmin<sup>-1</sup>, and the whole reaction time was just 100 min. As is shown in the graph, it is not difficult to see that they roughly have a uniform size. According to the findings, the size of the Ag NPs varied with the reaction time. In our study, the reaction can also be quenched at different reaction time to meet the diverse needs (Fig. S5B). It could be clearly concluded that the Ag NPs grow with the increasing of the reaction time and that the Ag NPs were uniform and pure from the synthesis procedures of different times. In conclusion, Ag NPs with a uniform morphology could be synthesized rapidly in less than 3.5 h, using a polyol process with zinc as the additive.

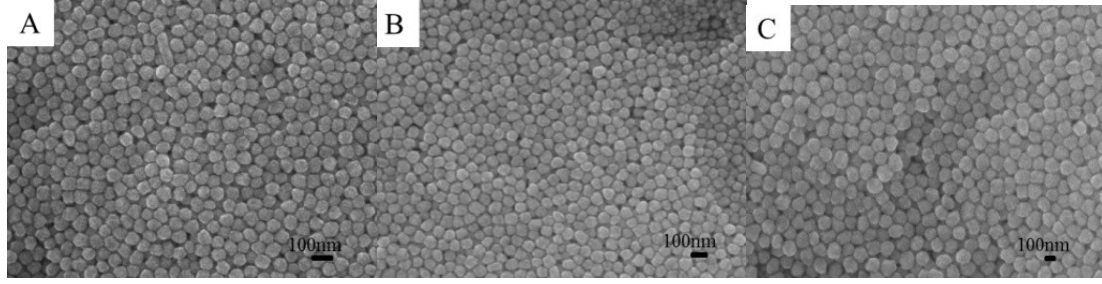


Fig. S5. SEM images of the Ag NPs synthesized with different reaction times at 140 °C with an agitation speed of 800 r min<sup>-1</sup>, with a reaction time of (A) 80 min (B) 120 min and (C) 150 min.

## S2. Effective indices of gap modes

It has demonstrated that the relationship between  $n_e$  and the spacer thickness,  $g$  can be said to be inversely proportional for very thin spacers so:  $\lambda_{pk} \sim n_e w \sim w/g$ . The dispersion relation for a NP-film waveguide can be written as eqn (3),

$$\tan\left(\frac{\alpha_d g}{2}\right) = -\frac{\varepsilon_m \alpha_m}{\varepsilon_d \alpha_d} \quad (3)$$

Where  $\alpha_{m,d} = \sqrt{k_{gsp}^2 - \varepsilon_{m,d} k_0^2}$  and  $k_0 = \frac{2\pi}{\lambda}$

Here  $k_{gsp}$  represents the surface plasmon-polariton (SPP) propagation constant. For small gapwidths, the approximation  $\tan h(x) \sim x$  can be used, which produces the expression:

$$k_{gsp} \approx k_0 \sqrt{\varepsilon_d + 0.5 \left(\frac{k_{gsp}^0}{k_0}\right)^2 + \sqrt{\left(\frac{k_{gsp}^0}{k_0}\right)^2 [\varepsilon_d - \varepsilon_m + 0.25 \left(\frac{k_{gsp}^0}{k_0}\right)^2]}} \quad (4)$$

Where  $\varepsilon_{d,m}$  are the spacer and metal bulk dielectric constants and  $k_{gsp}^0$  represents the SPP propagation constant in the limit of very narrow gaps, ( $t \rightarrow 0$ ) and is described as

eqn (3),  $k_{gsp}^0 = -\frac{2\varepsilon_d}{g\varepsilon_m(5)}$ . The effective index in the cavity,  $n_e$  is obtained via

$$n_e = \frac{Re[k_{gsp}]}{k_0} \quad (6).$$

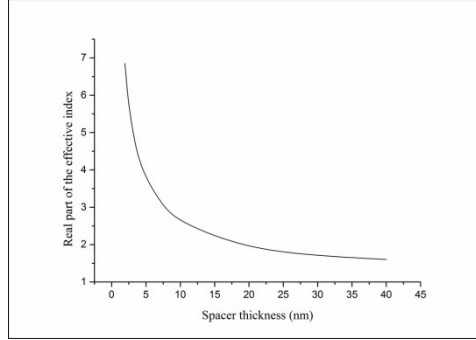


Fig. S6. Real part of the effective index of the guided mode inside the gap between the silver NPs and Au film as a function of the spacer thickness of the gap.

In this section, the physical behavior of the quasi-two dimensional structure (silver nanopolyhedrons on top of a gold film) is discussed in detail using Fourier Modal Method simulations<sup>30,38,39,40</sup>. The fundamental mode in a perfect air or dielectric filled metallic waveguide is a mode that presents no cutoff-it is supported whatever the thickness of the waveguide and the frequency considered. The fundamental mode is very often referred to as a coupled plasmon mode. Cavity resonances correspond to the build-up of a standing wave in the gap under the nanopolyhedrons. Such cavity

resonances can occur when the condition  $arg(r) + \frac{2\pi w}{\lambda_e} = m\pi$  (7) is satisfied,

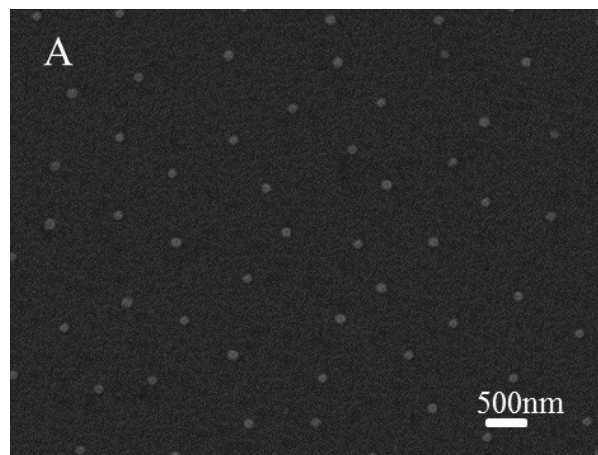
where  $m$  is an integer and  $r$  is the reflection coefficient of the mode at the end of the gap.

When the size of the nanopolyhedrons (the length of the cavity) is kept constant but the thickness of the gap changes, the variation of the wavelength  $\lambda_0$  for which a

resonance is excited satisfies  $\lambda_0 = n_e \frac{2\pi w}{m\pi - \arg(r)}$  (8). This means that the variation of  $\lambda_0$  reproduces exactly the variation of the effective index (provided the phase of the reflection coefficient can be considered as constant, which is usually the case) explaining the somewhat universal shape of the curve giving the position of the resonance as a function of the spacer thickness.

When the thickness of the spacer layer is decreased, the effective index,  $n_e$ , of the mode increases, and can reach arbitrarily large values. Because the relation between the resonance wavelength and the cavity size,  $l$ , is roughly  $l \approx \lambda/2n_e$ , resonances can thus be excited under nanopolyhedrons for which  $l$  is only one-tenth of the wavelength, especially for very thin spacer layers.

### S3. Scanning electronic microscopy images of surface coverage



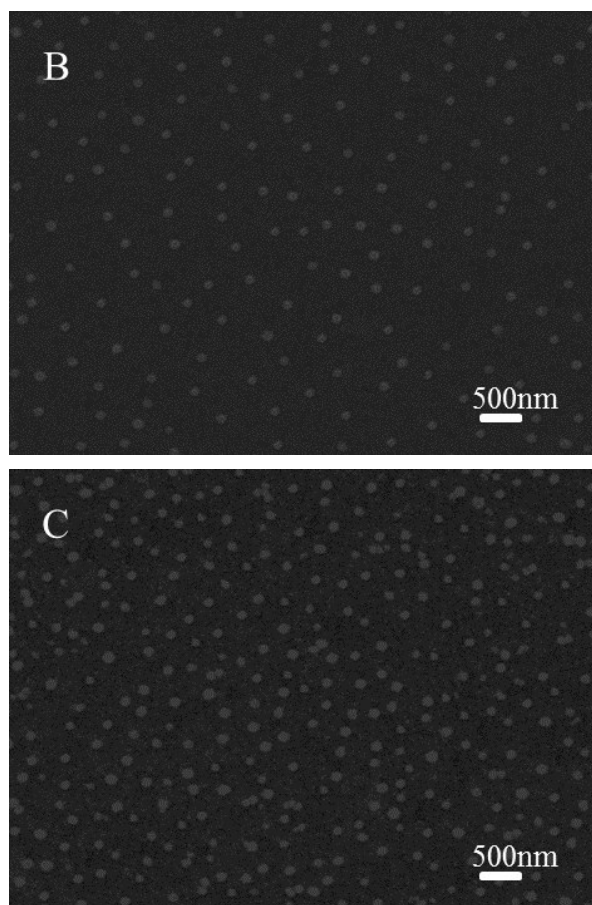


Fig. S7. Scanning electronic microscopy images of the silver nanocubes as fabricated and after deposition on the gold film with 3%, 15% and 30% surface coverage respectively.